Structure of a Dimeric BINOL-Imine-Zn(II) Complex and Its Role in Enantioselective Fluorescent Recognition

Kai Guo[a#], Ping Wang[a#], Wanli Tan[a#], Yan Li[a], Xiaowei Gao[a], Qin Wang*[a] and Lin Pu*[b]

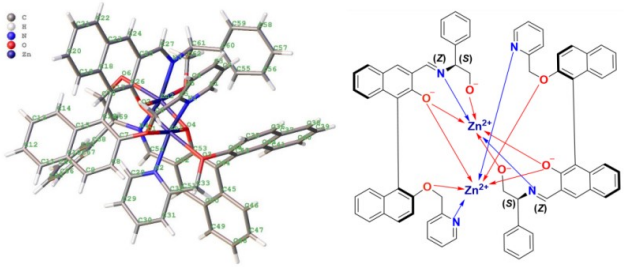

Abstract. A pyridine containing BINOL-based aldehyde (*S*)- or (*R*)-**4** is found to show highly enantioselective fluorescent response toward phenylglycinol in the presence of Zn^{2+}. A chirality matched dimeric BINOL-imine-Zn(II) complex is isolated from the reaction of (*S*)-**4** with L-phenylglycinol and Zn^{2+} whose structure is established by X-ray analysis. Comparison of the structure of this SS-complex with a molecular modeling structure of the chirality mismatched SR-complex generated from the reaction of (*S*)-**4** with D-phenylglycinol has provided important insight into the origin of the observed highly enantioselective fluorescent response. It is found that the solvent accessible surface area of the chirality-matched SS-complex is much smaller than that of the chirality mismatched SR-complex which gives the more tightly packed and structurally rigid SS-complex with greatly enhanced fluorescence.

Introduction

Enantioselective fluorescent recognition of chiral compounds has received significant attention in the past two decades.[1-3] The research in this area has not only provided fundamental knowledge about the molecular interaction of various probes with chiral substrates and their spectroscopic features, but can also lead to practical applications in rapid assay of chiral organic compounds as well as in optical imaging of biologically significant molecules. Our laboratory has used 1,1'-bi-2-naphthol (BINOL) to build fluorescent probes for the enantioselective recognition of various chiral molecules.[4] For example, we discovered that the BINOL-based aldehyde (*S*)-**1** in combination with Zn^{2+} showed enantioselective fluorescent enhancement when treated with chiral diamines, amino alcohols and amino acids (Figure 1).[5a] The bisBINOL compound (*R,R*)-**2** was later found to show highly enantioselective fluorescent responses toward common amino acids in the presence of Zn^{2+} in acetonitrile solution.[5b] Recently, we further found that compound (*R*)-**3** in combination with Zn^{2+} can be used to carry out the enantioselective fluorescent recognition of amino acids in neutral aqueous solution with near infrared excitation and emission.[6] Sasaki et al. also reported that the pyridine containing BINOL-aldehyde (*R*)-**4** in combination with Zn^{2+} can be used to discriminate the enantiomers of chiral diamines and amino alcohols in methanol solution.[7]

[a] Dr. Kai Guo, Ping Wang, Wanli Tan, Yan Li, Dr. Xiaowei Gao, Prof. Dr. Qin Wang
Key Laboratory of Medical Electrophysiology, Ministry of Education
School of Pharmacy of Southwest Medical University
Luzhou 646000, China
E-mail: wq_ring@hotmail.com

[b] Prof. Dr. Lin. Pu
Department of Chemistry, University of Virginia
Charlottesville, Virginia 22904-4319 (USA)
E-mail: lp6n@virginia.edu

# These authors contributed equally to this work.

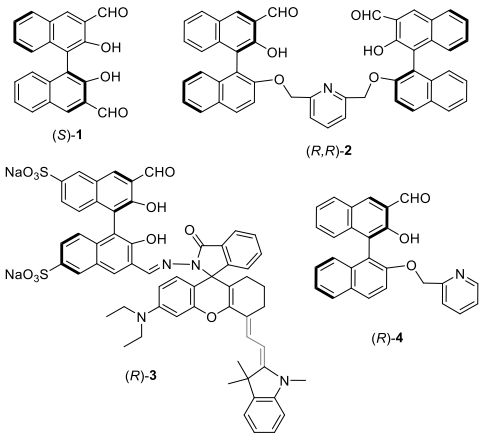

Figure 1. A few BINOL aldehyde-based fluorescent probes for enantioselective recognition of functional amines.

It has been proposed that when these BINOL-based aldehydes are used to react with the enantiomers of various chiral amines in the presence of Zn^{2+}, they should generate the corresponding diastereomeric BINOL-imine-Zn(II) complexes which contribute to the observed enantioselective fluorescent enhancement.[5-7] However, no crystal structure was obtained on such BINOL-imine-Zn(II) complexes before. Without the structural information of these complexes, the origin of the enantioselective fluorescent recognition of these probes remains elusive in spite of the significant work in this area. In order to achieve a better understanding on the BINOL+Zn(II)-based fluorescent probes in the molecular recognition of chiral functional amines, we have conducted a detailed investigation on the reaction of (*R*)- or (*S*)-**4** with the enantiomers of phenylglycinol. We have obtained the first X-ray structure of a BINOL-imine-Zn(II) complex which in combination with a molecular modelling study has provided significant insight into the fluorescent recognition process. Herein, our results are reported.

Results and Discussion

Study of the Fluorescent Response of (*S*)- and (*R*)-4 with $Zn(OAc)_2$ and Phenylglycinol.[7]

We prepared the two enantiomeric compounds (*S*)- and (*R*)-**4** starting from (*S*)- and (*R*)-BINOL according to a procedure developed in our laboratory (Scheme S1 in Supporting Information).[8] We then studied the fluorescent response of (*S*)-**4** toward L-/D-phenylglycinol in various solvents, including CH_2Cl_2, MeOH, EtOH, THF, MeCN, hexane and ^{i}PrOH (Figure S1c-r and Table S1). It was found that (*S*)-**4** has higher chiral recognition ability in CH_2Cl_2 and ^{i}PrOH than in other solvents and its fluorescence responses in ^{i}PrOH were more stable than those in CH_2Cl_2. As shown in Figure 2a and Figure S2, when an ^{i}PrOH solution of (*S*)-**4** (1.0×10^{-5} M) and $Zn(OAc)_2$ (1.0 equiv) was treated with L-phenylglycinol, a large fluorescence enhancement at $\lambda = 527$ nm was observed. The fluorescence intensity reached maximum when L-phenylglycinol was at 2 equiv with $I_L/I_0 = 308$ (Figure 2a). Under the same conditions, when the (*S*)-**4** and $Zn(OAc)_2$ solution was treated with the enantiomer D-phenylglycinol, the fluorescence enhancement was observed at a longer wavelength ($\lambda = 556$ nm) with much lower intensity ($I_D/I_0 = 36.8$). The fluorescent response of (*S*)-**4** toward L-/D-phenylglycine versus the reaction time was studied. It was found that the fluorescence enhancement of (*S*)-**4** by L-phenylglycine reached a stable plateau after 60 min and by D-phenylglycine after 80 min (Figure S3). Thus, a reaction time of 3 h was chosen for the fluorescence measurements in order to assure stable response. Figure 2b plots the fluorescence intensity at $\lambda = 527$ nm versus the concentration of L-/D-phenylglycinol. It shows that at 2 equiv of L-/D-phenylglycinol, (*S*)-**4** is a highly enantioselective fluorescent probe for the amino alcohol with the enantiomeric fluorescence enhancement ratio (ef) = 8.6 (ef = $[I_L-I_0]/[I_D-I_0]$).

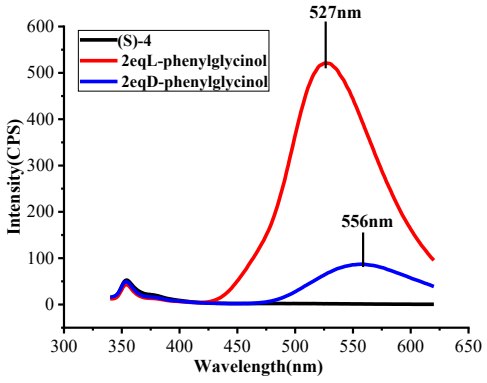

(a)

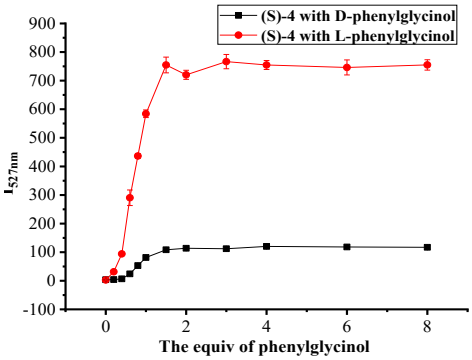

(b)

Figure 2. (a) Fluorescence spectra of (*S*)-**4** (1.0×10^{-5} M in ^{i}PrOH) + Zn^{2+} (1.0 equiv) in the presence of L-/D-phenylglycinol (2.0 equiv) (Reaction time: 3 h. $\lambda_{exc} = 320$ nm, slits: 5 nm/5 nm). (b) Fluorescence intensity I_{527} versus L-/D-phenylglycinol concentration (The error bars were obtained with three independent measurements).

We examined the fluorescent response of the enantiomeric probe (*R*)-**4** toward L-/D-phenylglycinol in ^{i}PrOH. As shown in Figure 3a and Figure S4, D-phenylglycinol produced much stronger fluorescent enhancement than L-phenylglycinol when they were interacted with (*R*)-**4** and Zn^{2+} (1.0 equiv) in ^{i}PrOH. The fluorescence intensity reached maximum when L-/D-phenylglycinol was at 2 equiv (Figure 3b), which demonstrates that these two enantiomeric probes (*S*)-**4** and (*R*)-**4** exhibit mirror image responses toward the amino alcohols. This confirms the enantioselectivity of these fluorescent probes.

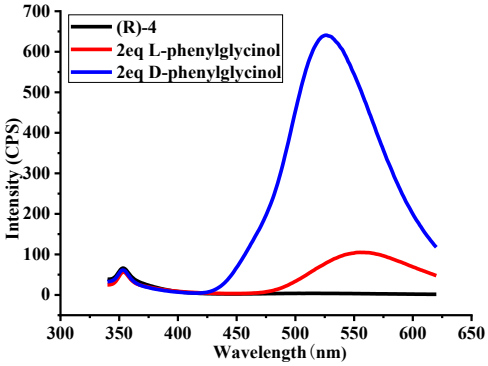

(a)

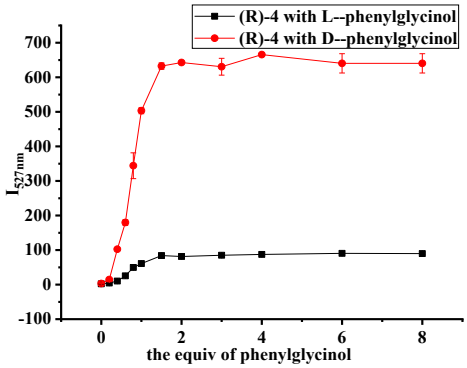

(b)

Figure 3. (a) Fluorescence spectra of (*R*)-**4** (1.0×10^{-5} M in ^{i}PrOH) + Zn^{2+} (1.0 equiv) in the presence of L-/D-phenylglycinol (2.0 equiv) (Reaction time: 3 h. $\lambda_{exc} = 320$ nm, slits: 5 nm/5 nm.) (b) Fluorescence intensity I_{527} versus L-/D-phenylglycinol concentration (The error bars were obtained with three independent measurements).

We then investigated the fluorescent response of (*S*)-**4** toward phenylglycinol of various enantiomeric compositions at a total concentration of 2.0×10^{-5} M. As shown in Figure 4, as the composition of L-phenylglycinol increased in the enantiomeric mixture, the fluorescence intensity at 527 nm increased. Thus, this fluorescent probe can be used to determine the enantiomeric composition of the amino alcohol.

We also studied the fluorescence response of (*S*)-**4** toward other amino alcohols including L-/D-phenylalaninol, prolinol,

alaniol, leucinol and valinol under the same conditions (Figure S5 in SI). There were different levels of fluorescence enhancement toward L-/D-amino alcohols, but the enantioselectivity was generally low.

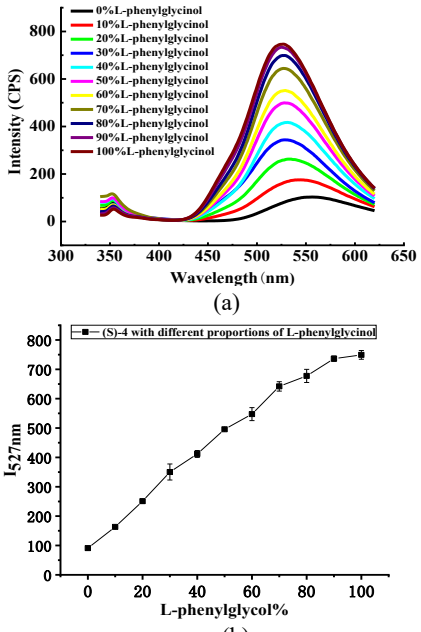

Figure 4. (a) Fluorescence spectra of (*S*)-**4** (1.0×10^{-5} M in ^{i}PrOH) + Zn^{2+} (1.0 equiv) with a mixture of L- and D-phenylglycinol (total concentration = 2.0×10^{-5} M) (Reaction time: 3 h; λ_{exc} = 320 nm, slits: 5 nm/5 nm). (b) Fluorescence intensity I_{527} versus L-phenylglycol composition (The error bars were obtained with three independent measurements).

Study of the Imine Products from the Reaction of (*S*)-4 with L- and D-Phenylglycinol

In order to understand the observed highly enantioselective fluorescent response of (*S*)-**4**, we prepared the two imine compounds (*S,S*)- and (*S,R*)-**5** from the condensation of (*S*)-**4** with L- and D-phenylglycinol respectively. As expected, when these two compounds were dissolved in ^{i}PrOH, little fluorescence was observed (Figure 5). When (*S,S*)-**5** was treated with $Zn(OAc)_2$ (1.0 equiv), there was large fluorescence enhancement at λ = 527 nm (Figure 5). However, when (*S,R*)-**5** was treated with $Zn(OAc)_2$ (1.0 equiv), a much smaller fluorescence enhancement was observed at λ = 556 nm. Thus, these two diastereomers exhibit very different fluorescence responses in the presence of $Zn(OAc)_2$, which are almost the same as those observed for the interaction of (*S*)-**4** with the amino alcohol enantiomers and $Zn(OAc)_2$ shown in Figure 2a. This supports the hypothesis that the enantioselective fluorescent responses of the probe (*S*)-**4** toward L-/D-phenylglycinol are due to the in situ formation of the diastereomeric imines and their subsequent interaction with $Zn(OAc)_2$.

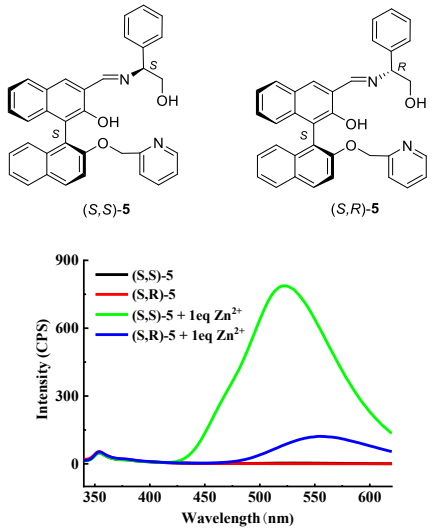

Figure 5. Fluorescence spectra of (*S,S*)-**5** or (*S,R*)-**5** (1.0×10^{-5} M) with/without $Zn(OAc)_2$ (1.0 equiv) in ^{i}PrOH. (Reaction time: 3 h. λ_{exc} = 320 nm. slits: 5 nm/5 nm.)

The reactions of compounds (*S,S*)- and (*S,R*)-**5** with $Zn(OAc)_2$ were investigated by ^{1}H NMR analysis. As shown in Figure 6a and Figure S6, when (*S,S*)-**5** was treated with $Zn(OAc)_2$ (1-2 equiv) in $CDCl_3/CD_3OD$ (1:5, v/v), it was completely converted to a new product with relatively sharp signals, indicating a well-defined structure. On the basis of the 2 D NMR spectra including COSY. NOSY and HMQC (Figure S6), the singlet at δ 8.10 of the Zn^{2+} complex in Figure 6a can be assigned to the imine proton, and the two doublets at δ 5.44 and 4.40 to the diastereotopic protons adjacent to the pyridine ring, the signals at δ 4.64 and 3.92 to the aliphatic protons of the phenylglycinol unit. When the diastereomer (*S,R*)-**5** was treated with $Zn(OAc)_2$ (1-2 equiv) under the same conditions, the resulting ^{1}H NMR signals are broad and complex, indicating a mixture of products with possibly fluxional structures (Figure 6b). Thus, the two diastereomeric imines formed very different products with $Zn(OAc)_2$.

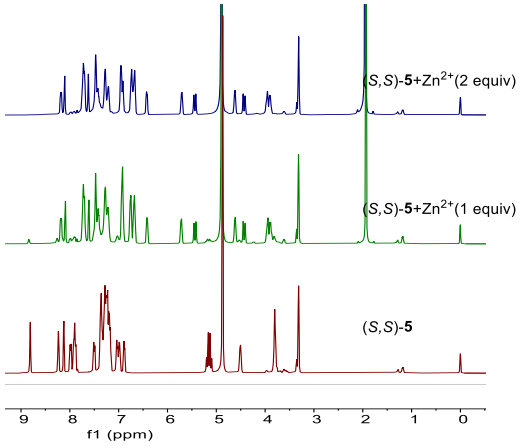

(a)

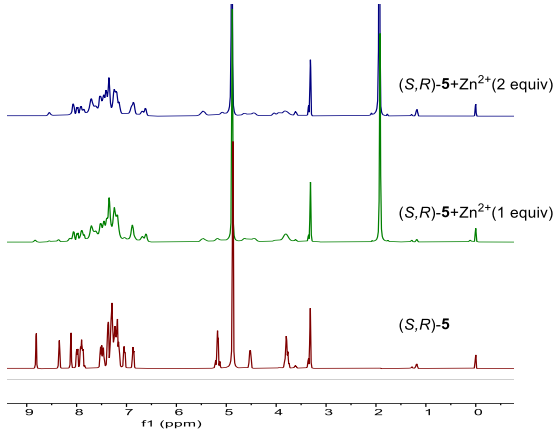

(b)

Figure 6. ^{1}H NMR spectra of (*S,S*)-**5** (a) and (*S,R*)-**5** (b) titrated with Zn^{2+} (0 - 2 equiv) in $CDCl_3/CD_3OD$ (1:5, v/v) for 6 h at room temperature.

The mass spectrum (ESI) of the reaction mixture of (*S*)-**4** with L-phenylglycinol (1 or 2 equiv) and $Zn(OAc)_2$ (1.0 equiv) in methanol was obtained (Figure S7c,d). Besides the signal for the imine product (*S,S*)-**5** [m/z (z = 1) = 525.22, calcd for (*S,S*)-**5**+H: 525.22], a significant peak at m/z (z = 1) = 1177.25 was observed which indicates the formation of a dimeric product [(*S,S*)-**5**+Zn]$_2$ (calculated for M+H = 1177.29). An intense peak at m/z (z = 2) = 589.13 was also observed for the dimer [(*S,S*)-**5**+Zn]$_2$ [calcd for (M+2H)/2 = 589.15]. However, the mass spectrum of the reaction mixture of (*S*)-**4** with D-phenylglycinol and $Zn(OAc)_2$ under the same conditions only gave mainly the signal of (*S,R*)-**5** with no signal for a stable zinc complex (Figure S7e,f). This demonstrates that the zinc complex generated from the coordination of (*S,S*)-**5** should be much more stable than that from (*S,R*)-**5**. That is, the reaction of (*S,S*)-**5** with Zn^{2+} gave a stable [2+2] dimeric complex [(*S,S*)-**5**+Zn]$_2$ with well-defined ^{1}H NMR signals but the reaction of (*S,R*)-**5** with Zn^{2+} gave only less stable complexes with broad ^{1}H NMR signals.

The excitation spectrum of (*S*)-**4** with Zn^{2+} and L-phenylglycinol shows two maxima at λ = 326 and 417 nm (Figure S1b). The shorter wavelength absorption at 326 nm can be attributed to the pyridylmethyl-substituted naphthoxyl unit of (*S,S*)-**5**, and the long wavelength absorption at 417 nm can be attributed to the naphthyl imine unit of (*S,S*)-**5** upon Zn^{2+} coordination because of the more extended conjugation. The observation that there is only one emission band at 527 nm suggests an efficient energy migration from the higher energy absorbing naphthoxy unit to the lower energy absorbing naphthyl imine unit of the zinc complex.

X-ray Structure of a BINOL-Imine-Zn(II) Complex and a Molecular Modelling Study

In order to gain more structural information for the dimeric zinc complex formed from the chirality matched interaction as discussed above, we devoted significant efforts to growing its single crystal. Since both $Zn(OAc)_2$ and $Zn(NO_3)_2$ in combination with (*S*)-**4** showed similar enantioselective fluorescent responses with phenylglycinol, they were used as the zinc ion sources to culture single crystals. After a series of experiments, we were delighted to obtain a single crystal from the reaction mixture of (*S*)-**4** with L-phenylglycinol (2.0 equiv) and $Zn(NO_3)_2$ (1.0 equiv) under the following conditions: (*S*)-**4** (406 mg), L-phenylglycinol (275 mg), and $Zn(NO_3)_2$ (298 mg) were dissolved in dichloromethane/methanol (1:1, 4 mL) in a 10 mL test tube. The solvent was evaporated slowly at 55 °C to give yellow crystals in 3 d. A single crystal with the following dimensions was chosen for X-ray analysis: 0.30 × 0.30 × 0.30 mm^3. The symmetry of the crystal structure was assigned the trigonal space group P32 with the following parameters: a = 14.06500(10) Å, b = 14.06500(10) Å, c = 27.9412(2) Å, α = 90 °, β = 90° , γ = 120° , V = 4786.91(8) Å3, Z = 3, Dc = 1.224 Mg/m3, F(000) = 1824.0, μ(Cu Kα) = 1.343 mm^{-1}, and T = 293(2) K.

As shown by the crystal structure in Figure 7a, the reaction generated a dimeric complex containing two (*S,S*)-**5** ligands and two zinc centers. This dimeric SS-complex shows a very interesting structure with an ingenious atomic arrangement. Through the coordination of the two ligands, both of the zinc centers have achieved a six-coordination with an octahedral geometry. All the five hetero atoms of the (*S,S*)-**5** ligand are coordinated to the zinc center in the dimeric structure. It is an electrically neutral binuclear complex containing neither counter ion nor hydrogen atom on the oxygen atoms coordinated to the Zn(II) centers (Figure 7b). As shown in Figure 8, the two ligands bite each other and bind tightly in the molecular surface with the two zinc ions surrounded in the center. It is inferred that this complex should have enhanced hydrophobicity.

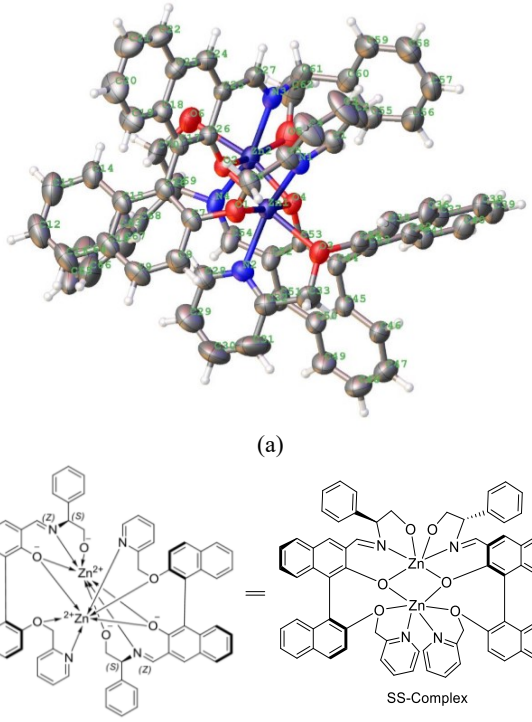

(a)

(b)

Figure 7. (a) The ORTEP structure (Showing 50% probability ellipsoids), and (b) ChemDraw representations of the SS-complex.

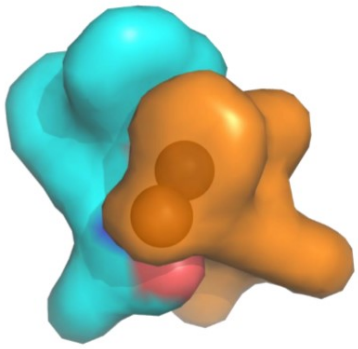

Figure 8. Schematic diagram of the molecular surface and center of the SS-complex from the X-ray structure [Left surface (blue-green) represents one ligand; Right surface (yellow-orange) represents another ligand; Center two brown circles represent two zinc ions; Pink represents oxygen atom; Blue represents nitrogen atom).

We conducted further molecular modelling study on the dimeric SS- and SR-complexes by using the Gaussian 09 d01 package,[9] with density functional theory (DFT) method at B3LYP level. It was found that the total energy of the SS-complex is -3498.02935 Hartree, and that of the SR-complex is -3497.79119 Hartree. Thus, the SS-complex is more stable than the SR-complex, and the energy difference is 149.45 kcal/mol. The greater stability of the SS-complex is attributed to its significant π-π stacking, which lowers the energy of the system. As shown in the structure of the SS-complex in Figure 9, its one naphthalene ring, a pyridine ring and another naphthalene ring form a sandwich type parallel stacking interaction with a plane distance of about 3.8 Å, but the SR-complex can only have a partial stacking interaction. In addition, the structure of the SS-complex is more closely packed through the stacking interaction, that is, the hydrophilic N and O atoms form coordination bonds with the zinc ions in the center while the hydrophobic benzene rings and naphthalene rings are exposed outside. The solvent accessible surface area of the SS-complex is calculated to be 1126.338 Å^2 and that of the SR-complex to be 1415.688 Å^2.[10] The significantly smaller solvent accessible surface area of the SS-complex indicates a much more tightly packed structure of this compound. This makes its central hydrophilic atoms less accessible by the polar solvent molecules in a polar solution, leading to a more rigid and stable structure with stronger fluorescence. In contrast, the SR-complex has a much bigger solvent accessible surface area and its structure should not be as tightly packed as the SS-complex. There will be more interaction of the central hydrophilic atoms with polar solvent molecules when the SR-complex is dissolved in a polar solution. This should lead to a more flexible and less stable structure with weaker fluorescence.

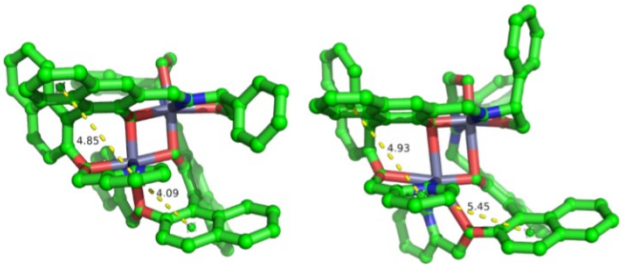

Figure 9. Structures of the SS-complex (left) and the SR-complex (right) to show the π-π stack interactions between the aromatic rings.

Figure 10 gives the frontier orbitals, including the highest occupied molecular orbital (HOMO) and the lowest unoccupied molecular orbital (LUMO), of the SS- and SR-complexes. The frontier orbital energy difference of the SS-complex is 2.596 ev, and that of the SR-complex is 2.538 ev (Table 1). It is found that the distribution of the HOMO of the SS-complex shows apparent difference from that of its LUMO, but the difference in the distributions of the HOMO and LUMO of the SR-complex is much smaller. For the SS-complex, the electron density contribution rate of 86.3% comes from two ligands in HOMO, but 87.1% only from *one* of the ligands in LUMO; for the SR-complex, 87.7% in HOMO and 85.5% in LUMO come from two ligands respectively. The SS-complex has a large conjugated π-π interaction as well as a rigid co-planar structure, which is conducive to the electronic transition from the high energy HOMO to the low energy LUMO with the large distribution differences when it is excited, contributing to the observed fluorescence enhancement at 527 nm.

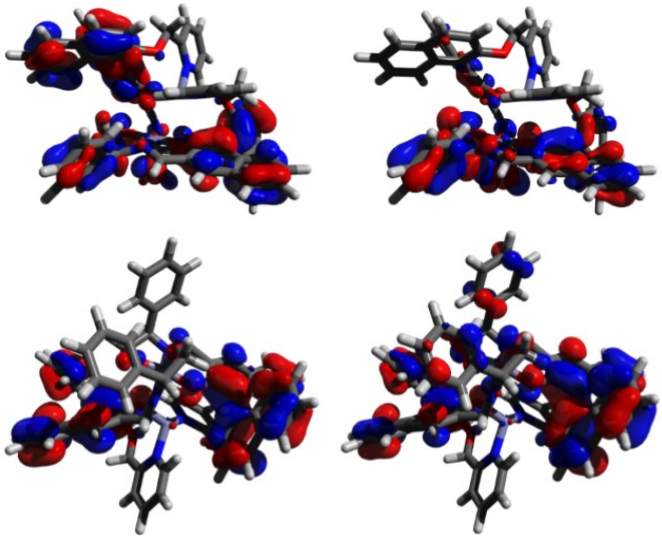

HOMO LUMO

Figure 10. Frontier molecular orbitals of the compounds (Up: The SS-complex. Down: The RS-complex)

Table1. The frontier orbital energy levels of the SS- and SR-complexes (unit: eV)

Compound	SS-complex	SR-Complex
HOMO	-4.736	-5.430
LUMO	-2.140	-2.892

Conclusions

In summary, we have demonstrated that the pyridine-containing BINOL aldehyde (*S*)- or (*R*)-**4** can be used as a highly enantioselective fluorescent probe for phenylglycinol in the presence of Zn^{2+}. On the basis of NMR and mass spectroscopic analyses, it is proposed that formation of an imine-Zn^{2+} complex from the condensation of the probe with the amino alcohol and Zn^{2+} and its subsequent stereoselective assembly to generate a chirality-matched dimeric complex is responsible for the greatly enhanced fluorescence for the chirality-matched interaction. We have obtained the crystal

structure of the chirality matched dimeric SS-complex formed from the reaction of (*S*)-**4** with L-phenylglycinol and Zn^{2+}. The X-ray structure of the SS-complex structure has allowed us to conduct a molecular modelling study and to compare the structure of the SS-complex with that of the chirality-mismatched SR-complex formed from the interaction of (*S*)-**4** with D-phenylglycinol and Zn^{2+}. The SS-complex is found to have a much smaller solvent accessible surface area than the SR-complex which is proposed to account for the much greater fluorescence of the SS-complex than that of the SR-complex. The SS-complex forms a tightly packed structure with a hydrophobic surface and a hydrophilic core which minimizes its interaction with polar solvent molecules to give greatly enhanced fluorescence. In contrast, the diastereomeric SR-complex has a much greater solvent accessible surface area with a less tightly packed structure. It is much easier for polar solvent molecules to interact with the hydrophilic core to destabilize the coordination of the ligand, giving reduced fluorescence. Thus, for the first time, a much more clear explanation can be provided for the highly enantioselective fluorescent responses of the BINOL-aldehyde-based probes toward chiral functional amines.

Although formation of dimeric BINOL-imine-Zn^{2+} complexes was previously proposed for the interaction of the BINOL-based compounds such as (*S*)-**1** with Zn^{2+} and amino acids on the basis of NMR and mass spectroscopic analyses,[11] no crystal structure was obtained and no detailed structural information was available. The discovery of the SS-complex in this work has significantly advanced our knowledge about this class of fluorescent probes which should facilitate their further development. This work not only contributes to the fundamental understanding of the molecular recognition process, but can also provide new ideas to design enantioselective fluorescent probes for applications in high throughput screening of asymmetric reactions as well as in fluorescent imaging of chiral molecules in biological systems.

Experimental Section

General Data. All ^{1}H and ^{13}C NMR spectra were recorded with a Bruker AVANCE III 400 MHz NMR spectrometer. Proton chemical shifts of NMR spectra were reported in ppm relative to TMS [$Si(CH_3)_4$] (0.00 ppm) as the internal reference. HRMS data were recorded on a SCIEX X500 QTOF mass spectrometer. Fluorescence spectra were obtained from a Hitech F-7000 spectrofluorometer. Optical rotations were acquired on a PerkinElmer M341 polarimeter. Unless otherwise noted, materials were obtained from commercial suppliers and were used without further purification. All of the solvents were HPLC grade in the optical spectroscopic studies.

Synthesis and characterization of (*S,S*)-5 and (*S,R*)-5. (*S*)-**4** (405 mg, 1.0 mmol) and D- or L-phenylglycinol (301 mg, 2.2 mmol) were placed in a 100 mL round bottom flask under nitrogen atmosphere. Dichloromethane (30 mL) was added to dissolve the solid, which was stirred overnight at room temperature. After complete reaction of (*S*)-**4**, the mixture was concentrated to 5 mL under vacuum and then slowly added into n-hexane (30 mL). Precipitate formed during the addition which was filtered and washed with n-hexane (5 mL). After dried, the products (*S,S*)-**5** (445 mg) and (*S,R*)-**5** (461 mg) were obtained as yellow solids in 85% and 88% yields respectively. *Characterization data of (S,S)-**5***: ^{1}H NMR (400 MHz, Chloroform-*d*) δ 13.00 (s, 1H), 8.76 (s, 1H), 8.38 (d, J = 9.0 Hz, 1H), 8.00 (s, 1H), 7.95 (d, J = 8.0 Hz, 1H), 7.90 (d, J = 8.0 Hz, 1H), 7.87 (dd, J = 8.0 Hz, 1H), 7.45 (dd, J = 12.0 Hz, 1H), 7.36-7.23 (m, 10H), 7.16 (bs, 1H), 7.14 (bs, 1H), 6.96 (dd, J = 8.0 Hz, J = 4.0 Hz, 1H), 6.87 (d, J = 8.0 Hz, 1H), 5.28 (dd, J = 12 Hz, 2H), 4.55 (dd, J = 8.0 Hz, J= 4.0 Hz, 1H), 3.89 (bs, 1H), 3.88 (s, 2H). ^{13}C NMR (120 MHz, Chloroform-*d*) δ 166.32, 157.67, 154.44, 154.01, 148.54, 139.00, 136.51, 135.59, 133.84, 133.78, 129.91, 129.76, 128.84, 128.84, 128.79, 128.40, 128.14, 127.96, 127.47, 127.25, 127.25, 126.66, 125.37, 124.99, 124.06, 123.44, 122.20, 120.93, 120.72, 119.85, 117.41, 115.96, 76.58, 72.09, 67.61. HRMS: m/z calcd. for $C_{35}H_{28}N_2O_3$ $[M+H]^+$: 525.2178, found: 525.2187. $[\alpha]^{20}_{(S,S)\text{-}5}$ = 137.7 (c = 1.0, CH_2Cl_2). *Characterization data of (S,R)-**5***: ^{1}H NMR (400 MHz, Chloroform-d) δ 13.03 (s, 1H), 8.74 (s, 1H), 8.38 (d, J = 9.0 Hz, 1H), 7.95 (s, 1H), 7.93 (d, J = 8.0 Hz, 1H), 7.86 (d, J = 8.0 Hz, 1H), 7.85 (d, J = 8.0 Hz, 1H), 7.45 (d, J = 12.0 Hz, 1H), 7.38-7.23 (m, 10H), 7.13 (bs, 1H), 7.11 (bs, 1H), 7.01 (dd, J = 8.0 Hz, J = 4.0 Hz, 1H), 6.79 (d, J = 8.0 Hz, 1H), 5.21 (dd, J = 12 Hz, 2H), 4.52 (dd, J = 8.0 Hz, J= 4.0 Hz, 1H), 3.87 (d, J=2.0 Hz, 1H), 3.85(s, 2H). ^{13}C NMR (120 MHz, Chloroform-*d*) δ 166.50, 157.77, 154.35, 153.77, 148.54, 139.08, 136.44, 135.69, 133.82, 133.82, 129.88, 129.53, 128.84, 128.84, 128.82, 128.46, 128.21, 127.97, 127.48, 127.21, 127.21, 126.70, 125.16, 125.06, 122.88, 123.49, 122.08, 120.90, 120.68, 119.13, 117.53, 115.00, 76.37, 71.40, 67.54. HRMS: m/z calcd. for $C_{35}H_{28}N_2O_3$ $[M+H]^+$: 525.2178; found: 525.2194. $[\alpha]^{20}_{(S,R)\text{-}5}$ = -108.8 (c = 1.0 Mm, CH_2Cl_2).

Sample Preparation for Fluorescence Measurement. All the stock solutions of (*S*)-**4** (1.0 mM, i-PrOH), L-/D-phenylglycinol (1.0 mM, i-PrOH) and $Zn(OAc)_2$ (2.5 mM, i-PrOH) were freshly prepared for each measurement. For fluorescence study, a solution of (*S*)-**4** was mixed with various equiv of the L-/D-phenylglycinol solution in a 10 mL test tube. The resulting solution was allowed to stand at room temperature for 3 h before being diluted with i-PrOH to the desired concentration [0.01 mM (*S*)-**4**]. All the fluorescence spectra were taken within 2 h.

Sample Preparation for NMR Measurement. A certain amount of (*S,S*)-**5** or (*S,R*)-**5** was weighed to prepare a 0.6 M deuterated methanol solution. Then 20 μL of the solution was added to a NMR tube to which 1 - 2 equiv of the zinc acetate solution (0.6 M, methanol) was added. After 8 h, the ^{1}H NMR spectra of the samples were acquired.

Computational Studies. The geometry of the SS-complex was acquired from the X-ray analysis, while that of the SR-complex was constructed by changing the connectivity of the chiral carbon atom. Geometry optimization were carried out by using the Gaussian 09 d01 package, with density functional theory (DFT) method at B3LYP level. The 6-31+g(d) basis set was used for C, N, O, H atoms and zinc atom was described by the effective core potential (ECP) LANL2DZ. Geometry and electronic properties were extracted from the optimized geometries.

AUTHOR INFORMATION

Corresponding Author

lp6n@virginia.edu (Lin Pu)

wq_ring@hotmail.com (Qin Wang)

ORCID

Lin Pu: 0000-0001-8698-3228

Qin Wang: 0000-0001-9852-5347

Notes

The authors declare no competing financial interest.

Supplementary Materials Available: Additional experimental description, fluorescence and UV spectra, molecular modeling data and X-ray analysis experiment. CCDC 1976654 contains the supplementary crystallographic data for this paper. These data can be obtained free of charge from The Cambridge Crystallographic Data Centre via www.ccdc.cam.ac.uk/structures.

Keywords: enantioselective, fluorescent recognition, amino alcohols, BINOL

Acknowledgement: LP thanks the partial support of the US National Science Foundation (CHE-1855443). QW thanks the support of Sichuan Science and Technology Program (2019JDTD0016) and the State Scholarship Fund (201708510004) from China Scholarship Council.

References

1. Pu, L. Fluorescence of Organic Molecules in Chiral Recognition. *Chem. Rev.* **2004**, *104*, 1687–1716.
2. (a) Leung, D.; Kang, S. O.; Anslyn, E. V. Rapid Determination of Enantiomeric Excess: A Focus on Optical Approaches. *Chem. Soc. Rev*. **2012**, *41*, 448–479. (b) Accetta, A.; Corradini, R.; Marchelli, R. Enantioselective Sensing by Luminescence. *Top. Curr. Chem*. **2011**, *300*, 175–216. (c) Zhang, X.; Yin, J.; Yoon, J. Fluorescence and Colorimetric Chemosensors for Fluoride-ion Detection. *Chem. Rev*. **2014**, *114*, 4918-4959.
3. Herrera, B. T.; Pilicer, S. L.; Anslyn, E. V.; Joyce, L. A.; Wolf, C. Optical Analysis of Reaction Yield and Enantiomeric Excess: A New Paradigm Ready for Prime Time. *J. Am. Chem. Soc*. **2018**, *140*, 10385-10401.
4. (a) Pu, L. Enantioselective Fluorescent Sensors: A Tale of BINOL. *Acc. Chem. Res*. **2012**, *45*, 150-163. (b) Pu, L. Simultaneous Determination of Concentration and Enantiomeric Composition in Fluorescent Sensing. *Acc. Chem. Res*. **2017**, *50*, 1032−1040.
5. (a) Huang, Z.; Yu, S. S.; Wen, K. L.; Yu, X. Q.; Pu, L. Zn(II) Promoted Dramatic Enhancement in the Enantioselective Fluorescent Recognition of Functional Chiral Amines by a Chiral Aldehyde. *Chem. Sci.* **2014**, *5*, 3457– 3462. (b) Zhu, Y.-Y.; Wu, X.-D.; Gu S.-X.; Pu, L. Free Amino Acid Recognition: a Bisbinaphthyl-Based Fluorescent Probe with High Enantioselectivity. *J. Am. Chem. Soc.* **2019**, *141*, 175-181.
6. Zhao, F.; Tian, J.; Wu, X.; Li, S.; Chen, Y.; Yu, S. S.; Yu, X. Q.; Pu, L. A Near-IR Fluorescent Probe for Enantioselective Recognition of Amino Acids in Aqueous Solution. *J. Org. Chem.* **2020**, *85*, 11, 7342-7348.
7. While our work on the reaction of (*S*)- and (*R*)-**4** with L- and D-phenylglycinol and $Zn(OAc)_2$ was in progress, the following paper on the interaction with other diamines and amino alcohols was reported: Sasaki, Y.; Kojima, S.; Hamedpour, V.; Kubota, R.; Takizawa, S.-y.; Yoshikawa, I.; Houjou, H.; Kubo, Y.; Minami, T. Accurate Chiral Pattern Recognition for Amines from just a Single Chemosensor. *Chem. Sci.* **2020**, 11, 3790-3796.
8. Wang, P.; Wang, Q. Identification of Amines with Fluorescent Probe of Binaphthol Derivatives. Master Degree Thesis of Southwest Medical University (Unpublished), **2018**, Chapter 1 Synthesis of Binaphthol Monoaldehyde Derivatives and Investigation of the Fluorescence Response of Chiral Amine Compounds.
9. (a) Becke, A. D. Density-functional thermo chemistry. I. The effect of the exchange-only gradient correction *J. Chem. Phys.*, **1992**, 96**,** 2155-60. (b) Petersson, G. A.; Bennett, A.; Tensfeldt, T. G.; Al-Laham, M. A.; Shirley, W. A.; Mantzaris, J. A complete basis set model chemistry. I. The total energies of closed-shell atoms and hydrides of the first-row atoms. *J. Chem. Phys.*, **1988**, *89*, 2193-218.
10. Hay, P. J.; Wadt, W. R. An initio effective core potentials for molecular calculations – potentials for the transition-metal atoms Sc to Hg. *J. Chem. Phys.*, **1985**, *82*, 270-83.
11. Song, T.; Cao, Y.; Zhao, G.; Pu, L. Fluorescent Recognition of Zn^{2+} by Two Diastereomeric Salicylaldimines: Dramatically Different Responses and Spectroscopic Investigation. *Inorg. Chem.* **2017**, 56, 4395-4399.

TOC Graph

The first X-ray structure of a dimeric BINOL-imine-Zn(II) complex was obtained, which has provided significant insight into the highly enantioselective fluorescent responses of the BINOL-aldehyde-based probes toward chiral functional amines. It was found that the solvent accessible surface area of the chirality-matched SS-complex is much smaller than that of the chirality mismatched SR-complex which gives the more tightly packed and structurally rigid SS-complex with greatly enhanced fluorescence.